CrossMark

ORIGINAL ARTICLE

The impact of land use and land cover change on net primary productivity on China's Sanjiang Plain

Guotao Dong[1,2] · Juan Bai[1,3] · Shengtian Yang[1] · Linna Wu[1] · Mingyong Cai[1] ·
Yichi Zhang[1] · Ya Luo[1] · Zhiwei Wang[1]

Abstract Land use and land cover change (LUCC) have a significant influence on regional ecosystems and on the carbon cycle. The Sanjiang Plain is one of the largest grain production bases in China, and has experienced rapid land cover change, making it a critical area in which to assess the environmental impact of LUCC and propose strategies for minimizing its impact on net primary productivity (NPP). In this study, land cover was estimated from remote sensing images to quantify LUCC on the Sanjiang Plain from 2000 to 2010. A moderate resolution imaging spectroradiometer dataset of photosynthetically active radiation absorbed by vegetation canopy, a land cover map, meteorological data and other field data were used to develop a CASA productivity model and obtain NPP for the study area. The spatial and temporal changes of NPP from 2000 to 2010 were then analyzed. Finally, the effect of LUCC on regional NPP was estimated. The land cover maps indicated that farmland expansion and wetland reduction were the most significant landscape changes on the Sanjiang Plain from 2000 to 2010. NPP loss totaled 2900 Gg (1 Gg = 10^9 g) of carbon from 2000 to 2005. By 2010, NPP had increased by at least 731 Gg of carbon, corresponding to 1184 Gg of net dioxide carbon sequestration. It was thus confirmed that LUCC has a significant, direct influence on regional NPP on the Sanjiang Plain.

Keywords Net primary productivity (NPP) · LUCC · CASA · Remote sensing-driven modelling · Sanjiang Plain

Introduction

Net primary productivity (NPP) is a key component of the terrestrial carbon cycle. NPP is the amount of solar energy converted into chemical energy through the process of photosynthesis (Imhoff et al. 2004), and represents the balance between accumulated photosynthesis and accumulated autotrophic respiration (Lieth and Whittaker 1975). In fact, NPP is the primary source of food for humans and other heterotrophic organisms. It is also a key input to the carbon budget, and can be seen as an indicator of ecosystem health. In agriculture, it nearly reflects grain yield. It is a key indicator that is widely used to estimate the levels of carbon uptake and respiration. NPP is a sensitive indicator of climatic and environmental changes (Schimel et al. 1997) and its changes may affect the atmosphere composition (Pimm and Raven 2000), biodiversity (DeFries et al. 1999), and energy adjustment mechanism (Houghton 2003).

Land use and land cover change (LUCC) and rapid population growth are occurring on a global scale. LUCC can directly affect the distribution and structure of terrestrial ecosystems, and can change the carbon cycle, which is the basis of the form of NPP reflect. The effect of LUCC on

Authors, G. Dong and J. Bai contributed equally to this article.

✉ Shengtian Yang
yangshengtian@bnu.edu.cn

1 State Key Laboratory of Remote Sensing Science, Jointly Sponsored by Beijing Normal University and the Institute of Remote Sensing Applications of Chinese Academy of Sciences, Beijing Key Laboratory for Remote Sensing of Environment and Digital Cities, School of Geography, Research Center for Remote Sensing and GIS, Beijing Normal University, Beijing 100875, People's Republic of China

2 Yellow River Institute of Hydraulic Research, YRCC, Zhengzhou 450003, People's Republic of China

3 College of Geographical Science, Shanxi Normal University, Linfen 041004, People's Republic of China

carbon in the terrestrial ecosystem has been studied at a variety of scales and in a number of regions. On a global scale, DeFries et al. (1999) used the Carnegie–Ames–Stanford Approach (CASA) model to estimate the effect of human-induced land cover change on global carbon emissions and NPP. Approximately 2 % of global terrestrial NPP was lost each year due to dryland degradation, or between 4 and 10 % of the potential dryland NPP (Zika and Erb 2009). On a regional scale, research has focused primarily on the Americas. Monthly carbon fluxes in terrestrial ecosystems of the Brazilian Amazon were found to be at least two times higher than previously recorded owing to forest deforestation (Potter et al. 2001). San José et al. (2008) revealed how land use changes affect NPP changes. Ahi et al. (2005) and Williams et al. (2005) assessed different land cover effects on NPP in a state of America. There is a smaller body of research from other regions. Quaife et al. (2008) suggested that terrestrial carbon fluxes were highly dependent on land cover in Western Europe. Luck (2007) studied the relationships between NPP and land use in Australia, and Xu et al. (2007) have assessed the impact of urbanization on regional NPP with satellite data and the BEPS process model in Jiangyin County, China.

Studying the impact of LUCC on NPP is crucial to understanding changes in the functioning and structure of the ecosystem and to predicting future trends. NPP is sensitive to climate, topography, soil, plant and microbial characteristics (Field et al. 1995). NPP varies geographically and over time, and cannot be observed directly at regional and global scales (Fang et al. 2003). Many models have been developed to estimate NPP based on different mechanisms, such as, the GLObal Production Efficiency Model (GLO-PEM) (Prince and Goward 1995), Terrestrial Uptake and Release of Carbon (TURC) (Ruimy et al. 1996), the Biome BioGeochemical Cycles model (BIOME-BGC) (Running et al. 2004), CENTURY (Parton et al. 1993), BIOME3 (Haxeltine and Prentice 1996), Boreal Ecosystem Productivity Simulator (BEPS) (Liu et al. 1997), and the Carnegie–Ames–Stanford Approach terrestrial carbon model (CASA) (Potter et al. 1993). The models can be divided into three categories (Ruimy and Saugier 1994): statistical, parameter, and process-based. The CASA model, based on light use efficiency (LUE) explored by Monteith (1972), is a process-based model and appropriate for estimating NPP on a global or regional scale. The CASA model is useful for describing spatial and temporal NPP features (Potter et al. 1993), and has been used as the effective model in global and regional spatial and temporal NPP estimations (Field et al. 1995; Cramer et al. 1999; Piao et al. 2001; Tao et al. 2005; Yu et al. 2009). Satellite-driven CASA based on moderate resolution imaging spectroradiometer (MODIS) remote sensing data has been used to simulate NPP. Remote sensing data have also been used to quantify the temporal NPP to provide information on the dynamics of biosphere production (Donmez et al. 2011).

Measures of NPP can quantify the impact of land transformation. However, the impact of LUCC on NPP on the Sanjiang Plain is poorly understood. Assessment of the impact is difficult because of limited available data and insufficient monitoring. Carbon cycle trends significantly influence the sustainability and security of ecosystems on the Sanjiang Plain. Understanding the impact of LUCC on NPP is thus crucial to predicting future carbon trends there. The primary objectives of this study are to estimate NPP change on the Sanjiang Plain by simulating spatial and temporal changes from 2000 to 2010 and to understand how, and to what extent, LUCC has affected NPP.

Study area

The Sanjiang Plain, located in the northeastern part of Heilongjiang Province (Fig. 1), has experienced some of the most dramatic land cover change in China. It is in a low alluvial plain of the Amur, Songhua, and Ussuri Rivers, from 129°11′E to 135°05′E, and from 43°49′N to 48°27′N, with a total area of 108,829 km². Its elevation in the southwest is higher than in the northeast. The climate is a temperate continental monsoon type with an annual mean temperature of 1.9 °C. The mean temperature in July and January is 22 and 21 °C, respectively. Water and soil in marshes are completely frozen from late October to April and begin to melt in late April. The annual mean precipitation is about 550–600 mm, concentrated in July and August, accounting for more than 60 % of the annual precipitation. Sanjiang Plain is the largest concentrated distribution area for freshwater marshes in China. Covered by a continuous clay layer, the Sanjiang Plain has a slope grade of about 1:5000–1:10,000, which is favorable for wetland formation.

Because the Sanjiang Plain is located in a border area, large areas of wetland still existed at the beginning of the 20th century. From the late 1950s to the early 1990s, with the influx of immigrants, the area of reclaimed farmland increased dramatically. A number of large farms, distributed throughout the plain, were built and are associated with the loss of wetlands. The plain is now one of China's primary food and agricultural bases. From the end of 1990s to 2010, a number of environmental restoration projects were conducted, and at the same time, dry lands were transformed into paddy fields in the interior farmlands. In 2003, the 69th Document of the Ministry of Land and Resource of the People's Republic of China issued a notification, the "National Land Consolidation and
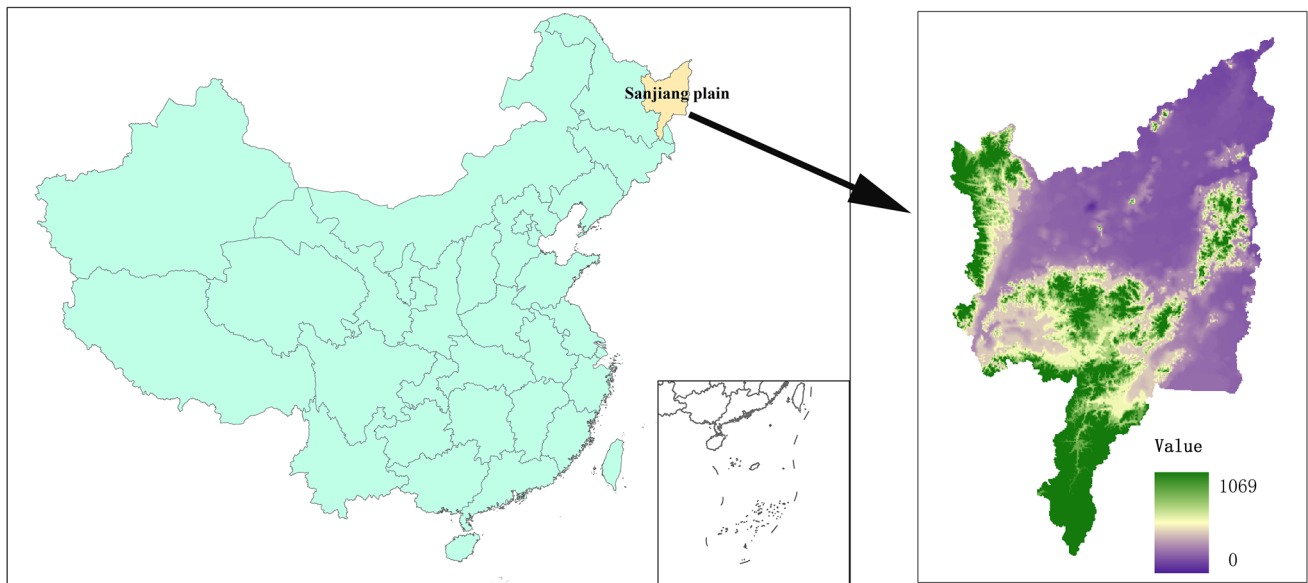
Fig. 1 Geographical location and DEM of Sanjiang Plain

Rehabilitation Plan", which outlined land development, consolidation and reclamation activities that were to be carried out on the Sanjiang Plain.

Materials and methods

NPP was estimated on a monthly time scale as the amount of absorbed photosynthetically active radiation (APAR) modulated by a LUE factor. The simulation method is based on the CASA model, and driven by MODIS remote sensing data. LUCC, and the FPAR data, were derived from MODIS.

CASA model

NPP at a grid cell (x) in time (t) is a product of APAR and LUE (ε) (Potter et al. 1993) (Eq. 1). The framework of the CASA model used to estimate NPP is shown in Fig. 2.

$$NPP(x,t) = APAR(x,t) \times \varepsilon(x,t) \qquad (1)$$

where NPP (x, t) represents NPP in the geographic coordinate of a given location x and time t. APAR (x, t) is the incident solar radiation absorbed by the vegetation (MJ m^{-2} month^{-1}); ε (x, t) is the LUE of the vegetation (g C MJ^{-1}).

APAR is determined by the product of the total incident solar radiation and the fraction of the incoming PAR intercepted by the green fraction of the vegetation (FPAR) (Eq. 2).

$$APAR(x,t) = SOL(x,t) \times FPAR(x,t) \times 0.5 \qquad (2)$$

where SOL (x, t) is the total incident solar radiation of a given location x and month t (MJ m^{-2}); FPAR (x, t) is the fraction of the total incoming PAR absorbed by vegetation canopy; 0.5 is the ratio of the effective solar radiation against the total solar radiation (wave length 0.4–0.7 μm). In this study, FPAR is obtained from MODIS-Terra 1 km 16-day FPAR products (MOD15), which were tested by Seixas et al. (2009).

$\varepsilon(x, t)$ is affected by a temperature and moisture factor, which can be expressed by the following equation:

$$\varepsilon(x,t) = T_{\varepsilon 1}(x,t) \times T_{\varepsilon 2}(x,t) \times W_{\varepsilon}(x,t) \times \varepsilon_{max} \qquad (3)$$

where $T1$ (x, t) and $T2$ (x, t) account for temperature stress coefficients; $W(x,t)$ is the moisture stress coefficient; ε_{max} is the maximum LUE of the specific biome under ideal conditions.

Potter et al. (1993) set the maximum LUE at 0.389 g C MJ^{-1} for various vegetation types in the CASA model. However, this value can be affected by a series of environmental factors, such as soil type, temperature, water availability, plant nutrition, and ecosystem energy distribution (Prince 1991). These factors interact with one another, and create a wide variation in value (ε) in the real world (Paruelo et al. 1997; McCrady and Jokela 1998). Moreover, a number of studies that employed the CASA model to estimate NPP have shown that the value of 0.389 g C MJ^{-1} would underestimate simulated NPP (e.g., Running et al. 2000; Peng 2000). In this study, the findings of Zhu et al. (2006) regarding the maximum LUE values for different vegetation types were applied.
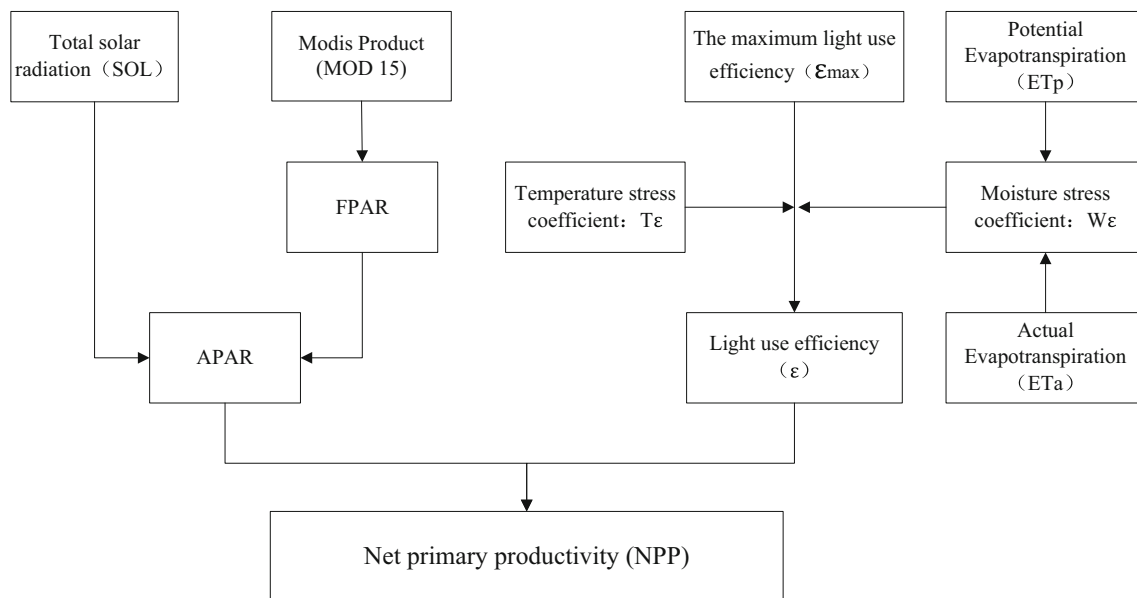
Fig. 2 The framework of CASA estimate NPP

The two temperature stress terms serve to depress ε at very high and very low temperatures and to depress ε when the temperature is above or below the optimum temperature (T_{opt}), where $T_{opt}(x)$ is defined as the air temperature in the month when the NDVI reaches its maximum for the year. $T_{opt}(x)$ ranges from near 0 °C to the mid thirties in low latitude deserts.

$T_{\varepsilon 1}(x)$, which ranges from 0.8 at 0 °C to 1.0 at 20 °C to 0.8 at 40 °C, is described as (Potter et al. 1993)

$$T_{\varepsilon 1} = 0.8 + 0.02T_{opt} - 0.0005T_{opt}^2 \qquad (4)$$

where $T_{opt}(x)$ is defined as the air temperature in the month when the NDVI reaches its maximum for the year. When mean monthly temperature is -10 °C and below, $T_{\varepsilon 1}(x)$ is set to zero.

$T_{\varepsilon 2}$ reflects the concept that the efficiency of light utilization should be depressed when plants are growing at temperatures displaced from their optimum, and has an asymmetric bell shape that falls off more quickly at high than at low temperatures. It is calculated as (Potter et al. 1993):

$$T_{\varepsilon 2}(x,t) = 1.1814 \Big/ \left\{ 1 + e^{[0.2(T_{opt}(x)-10-T(x,t))]} \right\} \Big/ \\ \left\{ 1 + e^{[0.3(-T_{opt}(x)-10-T(x,t))]} \right\} \qquad (5)$$

$T_{\varepsilon 2}$ falls to half its value at T_{opt} at temperatures of 10 °C above or 13 °C below T_{opt}. The idea behind including $T_{\varepsilon 2}$ is to capture some of the intrinsic limitations on the flexibility of temperature acclimation.

The water stress factor (W_{ε}) is given by:

$$W_{\varepsilon} = 0.5 + 0.5ET_a(x,t)/ET_p(x,t) \qquad (6)$$

where ET_a is actual evapotranspiration (mm), ET_p is potential evapotranspiration (mm). ET_a and ET_p come from the soil moisture submodel. W_{ε} varies from 0.5 in very arid ecosystems to 1 in very wet ecosystems (Piao et al. 2001). When ET_a is greater than ET_p, W_{ε} equals 1. When months have a mean temperature less than or equal to 0 °C, W_{ε} the value from the previous monthly time step is carried forward without change. In this study, the ET_a and ET_p are calculated according to the Penman–Monteith (P–M) method recommended by the Food and Agriculture Organization (FAO) (Allen et al. 1998). The all computation data required to calculate ET_0 followed the recommendations of the FAO (Allen et al. 1998). The moisture stress factor is simultaneously related to many soil parameters, such as field moisture capacity, wilting coefficient, the percentage of soil sand and clay particles, and depth of soil.

Data sources

Data sources included remote sensing data, basic geographical data, meteorological data and other data. We chose a combination of satellite data, geo-spatial meteorological data and ground observational data of NPP for the study. All data were reproduced at 1×1 km spatial resolution and projected to Albers, using World Geodetic System-84 (WGS84) datum. The spatial databases regarding the topography, land use, and soil properties were developed and reclassified for the model. The time scale of the whole model is monthly.

The land cover map was compiled from MODIS (2000–2010) images and FPAR data were from MODIS/

Terra 1 × 1 km 16-day FPAR (MOD15) data from 2000 to 2010. The data were downloaded through EOS Data Gateway at the Land Processes Distributed Active Archive Center. The MODIS/Terra 16-day FPAR data were reproduced to monthly data by linear interpolation. We used land cover maps both to track land cover changes due to LUCC and to estimate NPP. Land cover in 2000 was acquired from Landsat Thematic Mapper TM; land-cover information for 2005 was acquired from China-Brazil Earth Resources Satellite (CBERS-1) data, and land-cover information for 2010 was acquired from MODIS data. Land cover maps for 2000, 2005 and 2010 were developed showing seven land cover types: (1) wetland, (2) cropland, (3) woodland, (4) grassland, (5) water body, (6) residential land, and (7) barren land. The cropland was divided into dry land and paddy field two types, which were the typical features of maize and rice farming, respectively. The accuracy of the 2000 and 2005 land cover maps interpreted from remote sensing images exceeded 87 % (89.7 % for 2000, and 92.6 % for 2005) (Song et al. 2008; Dong et al. 2013). The land cover maps were then re-sampled to a 1 × 1 km spatial resolution, and used to describe the extent and spatial distribution of land cover changes caused by LUCC on the Sanjiang Plain from 2000 to 2010. The land cover map of 2000 represents land cover in the period 2000–2003. The land cover map of 2005 represents land cover in the period 2004–2007. The land cover map of 2010 represents land cover in the period 2008–2010.

Meteorological input data were obtained from the 22 weather stations on the interior and surrounding the Sanjiang Plain. The climate data include mean monthly temperature, mean monthly precipitation and sun radiation data from 2000 to 2010. The data were bilinearly interpolated into an image with 1 km × 1 km resolution to match MODIS data.

The soil map is based on digitized soil maps with a scale of 1:1,000,000 (http://www.soil.csdb.cn). Soil texture data were based on the seven classes of the FAO soil texture classification. The dominant soil type in a soil unit was determined by the relative amounts of clay, silt, and sand present in the top 30 cm of soil.

We used these data to interpolate climate data for each individual pixel on the Sanjiang Plain with the GIS platform. We calculated NPP using the MODIS-based FPAR data as the input to the CASA productivity model to evaluate the effect of LUCC.

Results and discussion

Model validation

Some statistical crop yield data were collected to validate the precision of the model results. Simulated NPP in each county was calculated using a GIS statistical module and then comparing it with the crop yield in the statistical yearbook. Because the statistical material concerns crop seed yield, it was converted to NPP (including seed, straw, and roots) using the crop harvest index.

Steps followed to convert the harvestable product into NPP at the district level included: (1) conversion from reporting crop-product units of yield to units of mass; (2) conversion from fresh weight to dry weight using the crop values of moisture content (MC); (3) estimation of above-ground biomass using crop harvest indices (HI), defined as the ratio of economic product (e.g., grain) dry weight to plant above-ground dry weight; and (4) estimation of below-ground biomass as a function of above-ground biomass. Following Lobell et al. (2002), we assume that 45 % of crop biomass is C and above-ground biomass accounts for 80 % of total crop biomass. The cropland NPP is thus expressed as gram C per unit area and is calculated as:

$$\text{NPP}(\text{g C m}^{-2}) = \sum_{i=1}^{N} \frac{Y_i \times \text{MY}_i \times (1 - \text{MC}_i) \times 0.45 \frac{gC}{g}}{\text{HI}_i \times 0.9} \Bigg/ \sum_{i=1}^{N} A_i \tag{7}$$

where, Y_i is the reported production for crop i, MY_i is the mass per unit of harvestable product, A_i is the harvest area of crop i. The numerator and denominator are summed over $N = 7$ crops. The values of MC_i and HI_i of different crops were obtained from the literature and are listed in Table 1 (Lobell et al. 2002; Guo et al. 2009). The results of the comparison were analyzed using SPSS software to determine the precision of our results.

A shortage of real measurements of vegetation NPP led to the selection of measurements of the total crop yield recorded in the statistical yearbook for each county for the validation. Total crop yields for 22 counties in Jiamusi, Hegang, Shuangyashan, Qitaihe, Jixi and Harbin were selected from the statistical yearbook. Regression results demonstrated that there was a strong relationship between simulated NPP based on the CASA model and the NPP inversed from census at the county level (Fig. 3; $R^2 = 0.842$). The slope of this relationship was 0.764,

Table 1 Harvest index and moisture content of major crops

Crop	Harvest index	Moisture content (%)
Paddy	0.45	14
Maize	0.46	13
Beans	0.25	12.5
Wheat	0.40	12.5
Sorghum	0.40	10
Tubers	0.50	80
Peanut	0.40	9

indicating that the NPP values based on the cropland census were greater than the simulated values.

The calculated NPP was in accordance with that of Luo et al. (2010), who estimated the NPP based on MOD17A3 (with spatial resolution of 1×1 km) for Songnen Plain and found that mean dry land NPP in this region ranged from 280 to 310 g Cm^{-2}, and mean paddy field NPP ranged from 299 to 327 g Cm^{-2}. Forest NPP in 2000 and 2005 was 519 and 447 g Cm^{-2}, which was comparable to results obtained by Zhu et al. (2007) and He et al. (2005). Grassland and wetland NPP was also comparable to similar previous studies (Piao et al. 2001, 2005; Chen et al. 2007). The results of Zhang and Zhou (2008) study in the Northeast China Transect (NECT) found that forest NPP was 564 g Cm^{-2}; grassland NPP was 432 g Cm^{-2}. We found that forest NPP was 466 g Cm^{-2} and grassland was 412 g Cm^{-2}. This is likely because the Sanjiang Plain is in the north of the NECT area, where solar radiation and NPP are relatively higher. We conclude that the CASA model is suitable for NPP estimation on the Sanjiang Plain.
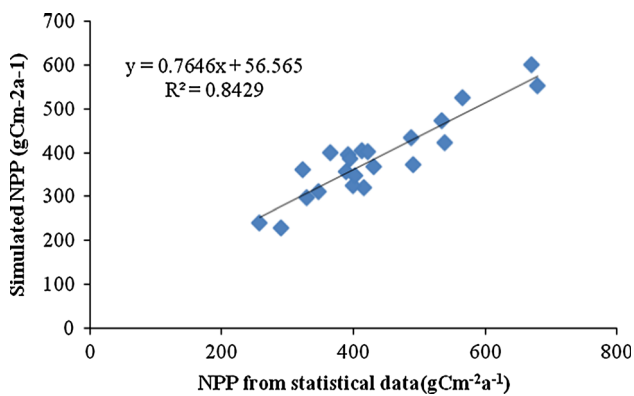

Fig. 3 Comparison between simulated NPP with NPP based on county statistics

Land cover changes based on remote sensing

The land use and land cover maps for 2000, 2005, and 2010 produced from MODIS images are shown in Fig. 4. The overall land use changes from 2000 to 2010 are shown in Tables 2 and 3. According to the two tables, dry land and forest were the two largest land-use types in this region from 2000 to 2010. Dry land constituted 40.64, 41.61, and 41.83 % of the total area, and forest was 31.20, 29.89, and 28.01 %, of the total area in 2000, 2005 and 2010, respectively. From Table 2 we can see that the areas of paddy field, dry land and residential land increased from 2000 to 2010. On the contrary, the areas of forest and wetland decreased.

The most notable changes in land use on the Sanjiang Plain were a decline in wetland and an increase in farmland. In 2000, wetland covered about 9.65 % of the study area, with an estimated total area of 10,504 km^2, but by 2010, the total area of wetland was estimated to have decreased by about 33 %, to 7075 km^2. The annual rate of decrease slowed from 3.6 % $year^{-1}$ in 2000 and 2005, to 2.8 % $year^{-1}$ in 2005 and 2010. Meanwhile, paddy fields increased by about 53 %, from 11,420 km^2 in 2000 to 17,451 km^2 in 2010, with an annual growth rate of 3.2–6.8 %.

In 2000, grassland covered about 3.88 % of the study area, with an estimated total area of 4220 km^2. By 2005, the total area of grassland decreased to 2616 km^2, but by 2010, grassland was estimated to have decreased by about 31 %, to 2931 km^2. While the size of this category decreased by 38 % between 2000 and 2005, it appeared to increase by about 12 % between 2005 and 2010.

Forest decreased slightly, from 33,956 to 30,478 km^2, with an annual reduction rate of 0.8–1.3 % from 2000 to 2010. Residential land, on the other hand, increased in size, from 2246 to 2499 km^2, with an annual reduction rate of
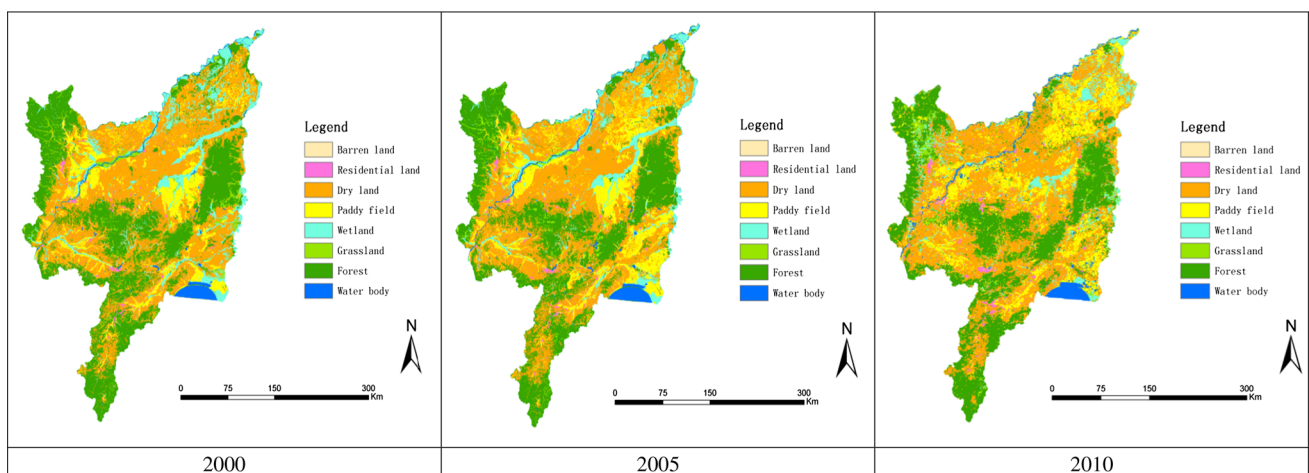

Fig. 4 Land use and land cover maps for 2000, 2005, and 2010

Table 2 Total area and area changes of land use types from 2000 to 2010

Land use type	Total area (km^2)			Area (%)		
	2000	2005	2010	2000 (%)	2005 (%)	2010 (%)
Forest	33,956	32,524	30,478	31.20	29.89	28.01
Grassland	4220	2616	2931	3.88	2.40	2.69
Dry land	44,224	45,274	45,519	40.64	41.61	41.83
Paddy field	11,420	15,016	17,451	10.49	13.80	16.04
Wetland	10,504	8590	7075	9.65	7.89	6.50
Water body	2183	2355	2758	2.01	2.16	2.53
Residential land	2246	2336	2499	2.06	2.15	2.30
Barren land	64	106	106	0.06	0.10	0.10
	108,817	108,817	108,817	100	100	100

Table 3 Estimated areas of each land use and land use changes from 2000 to 2010

Land use category	2000–2005			2005–2010		
	km^2	%	%/year	km^2	%	%/year
Forest	−1432	−4.2	−0.8	−2046	−6.3	−1.3
Grassland	−1604	−38	−7.6	315	12	2.4
Dry land	1050	2.4	0.48	245	0.5	0.1
Paddy field	3596	31.5	0.63	2435	16.2	3.2
Wetland	−1914	−18.2	−3.6	−1515	−17.6	−3.5
Water body	172	7.9	1.6	403	17.1	3.4
Residential land	90	4	0.8	163	7	1.4
Barren land	42	65.6	13.1	0	0	0

0.8–1.4 % from 2000 to 2010. Barren land, including abandoned cropland, sand land, and wasted grassland, increased by 65.6 % from 2000 to 2010. Bodies of water were estimated to increase from 2183 km^2 in 2000 to 2355 km^2 in 2005 and to 2758 km^2 in 2010. It is notable that, while the size of this category increased by 7.9 % between 2000 and 2005, it appeared to increase by about 17.1 % between 2005 and 2010.

Spatial NPP change from 2000 to 2010

The variation of NPP on the Sanjiang Plain from 2000 to 2010 is shown in Fig. 5. For the total area, the time series was divided into three periods: the first 4 years (2000–2003) (T1), middle four years (2004–2007) (T2) and last 3 years (2008–2010) (T3). The peak values of vegetation NPP are mainly distributed in central and western mountains and the southeastern hilly areas, accounting for more than 30 % of the entire area. Because of the abundance of arable land in the plains region, and because farmland NPP is lower than it is in the forest, the NPP value in the plain region was lower than in the hilly areas. However, there were a number of wetlands in the plain region and their NPP is high. Vegetation NPP in the

plain region along a river or wetland thus had a high value. Figure 5 shows that the natural vegetation in the western and central area has a decreased NPP value, whereas the majority of the cultivated vegetation area in the middle and north has increased NPP values from 2000 to 2010. Most of the variation percentage is from 5 to 20 %, as a result, within a some variation scope. As mentioned above, water conditions in T2 have gradually deteriorated, which has damaged the natural vegetation and led to decreasing NPP values. On the contrary, the cultivated vegetation's NPP increased. This indicates that natural vegetation growth is more influenced by climate conditions than is cultivated vegetation.

Results showed a mean NPP for each land cover type that decreased during the 10-year period. In this period, net primary production for the entire Sanjiang Plain decreased from 4.37×10^4 to 4.1×10^4 Gg C (1 Gg = 10^9 g). Regional total primary production thus decreased by 2575 Gg C or 5.9 % of the net primary production in 2000.

Impact of LUCC on NPP change

Estimated value of mean and total NPP in T1 and T2, and T2 and T3 for the Sanjiang Plain are shown in Tables 4 and 5.
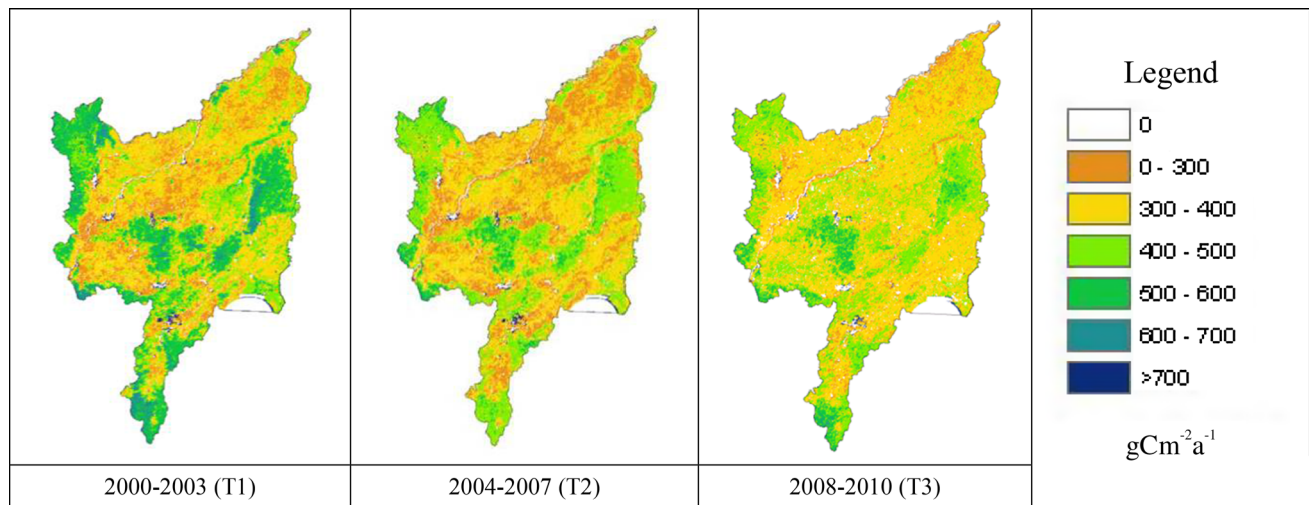
| 2000-2003 (T1) | 2004-2007 (T2) | 2008-2010 (T3) |

Fig. 5 Variation of NPP in Sanjiang Plain from 2000 to 2010

Table 4 Estimated value of mean and total NPP in 2000–2003 (*T*1) and 2004−2007 (*T*2) for Sanjiang Plain

Land cover	Mean NPP (g Cm^{-2} a^{-1})		Unit change (g Cm^{-2})	Percent change (%)	Total NPP (Gg C)		Total change (Gg C)	Percent change (%)
	*T*1	*T*2			*T*1	*T*2		
Forest	497.3	458.7	−38.6	−7.8	1.69×10^4	1.49×10^4	-0.2×10^4	−11.8
Grassland	431.7	410.4	−21.3	−4.9	0.18×10^4	0.11×10^4	-0.07×10^4	−38.9
Dry land	345.3	327.7	−17.6	−5.1	1.53×10^4	1.48×10^4	-0.05×10^4	−3.3
Paddy field	404.5	390.1	−14.4	−3.6	0.46×10^4	0.59×10^4	0.13×10^4	28.3
Wetland	432.6	416.8	−15.8	−3.7	0.45×10^4	0.36×10^4	-0.09×10^4	−20
Total	–	–	–	–	4.31×10^4	4.03×10^4	-0.28×10^4	−6.5

The impact of LUCC on NPP change was estimated by land use changes in three periods. Mean net primary production for the Sanjiang Plain was 422.3 g Cm^{-2} in *T*1, 400.7 g Cm^{-2} in *T*2, 410 g Cm^{-2} in *T*3. The largest NPP loss (38.6 g Cm^{-2}) occurred in forest areas. NPP loss in grassland and dry land areas was 21.3 and 17.6 g Cm^{-2}, respectively. Annual NPP in the total Sanjiang Plain was 4.37×10^4 Gg C in *T*1; annual NPP was 4.0×10^4 Gg C in *T*2 and 4.1×10^4 Gg C in *T*3. It is a concern that the mean NPP for wetland areas decreased consistently from 432.6 to 416.8 g Cm^{-2}, and then declined further to 414.2 g Cm^{-2}.

During the *T*1 and *T*2 periods, mean NPP for the total area of the Sanjiang region decreased from 422.3 to 400.7 g Cm^{-2}. Among all land cover types, forest NPP decreased the most, about 7.8 %, while paddy fields decreased about 3.6 %. Annual NPP of forest in *T*1 was the largest, about 1.69×10^4 Gg C, and made up 39.2 % of the total NPP. The mean NPP for forest decreased from 497.3 to 458.7 g Cm^{-2} from *T*1 to *T*2. The mean NPP for paddy decreased from 404.5 to 390.1 g Cm^{-2} from *T*1 to *T*2. However, total NPP increased from 0.46×10^4 to

0.59×10^4 Gg (28.3 %) from *T*1 to *T*2 due to the expansion of paddy fields.

The situation is quite different during *T*2 and *T*3, however. During the *T*2 and *T*3 periods, mean NPP for the total area of the Sanjiang region increased from 400.7 to 410 g Cm^{-2}. As the forest area shrank, total NPP decreased from 1.49×10^4 to 1.48×10^4 Gg (1 %) from *T*2 to *T*3. Mean forest NPP increased from 458.7 to 484.5 g Cm^{-2} from *T*2 to *T*3, indicating that forest quality per area improved from 2004 to 2010. During *T*2 to *T*3, forest NPP decreased by 33.06 and 17.8 %, respectively, mainly caused by timber harvesting; this trend was reversed in 2008.

Influencing factors of NPP on the Sanjiang Plain

There are many factors that could influence regional NPP, such as climate (solar radiation, temperature, and precipitation), land use and land cover, soil type, and human activities. As a result of the area increasing by 3596 km^2, even while mean paddy field NPP decreased, the total paddy field NPP increased by 0.13×10^4 Gg C from *T*1 to

Table 5 Estimated value of mean and total NPP in 2004–2007 (T2) and 2008–2010 (T3) for Sanjiang Plain

Land cover	Mean NPP (g Cm^{-2} a^{-1})		Unit change (g Cm^{-2})	Percent change (%)	Total NPP (Gg C)		Total change (Gg C)	Percent change (%)
	T2	T3			T2	T3		
Forest	458.7	484.5	25.8	5.6	1.49×10^4	1.48×10^4	-0.01×10^4	−1.0
Grassland	410.4	421.5	11.1	2.7	0.11×10^4	0.12×10^4	0.01×10^4	15.1
Dry land	327.7	332.2	4.5	1.4	1.48×10^4	1.51×10^4	0.03×10^4	1.9
Paddy field	390.1	397.8	7.7	2	0.59×10^4	0.7×10^4	0.11×10^4	18.5
Wetland	416.8	414.2	−2.6	−0.6	0.36×10^4	0.29×10^4	-0.07×10^4	−18.1
Total	–	–	–	–	4.03×10^4	4.1×10^4	0.07×10^4	1.7

T2. With this exception, land cover total NPP decreased overall, and total NPP on the Sanjiang Plain decreased by 6.5 % compared to that in T1. Meanwhile, the area of dry land increased, but the total dry land NPP decreased from T1 to T2. This development calls for immediate attention.

Annual mean temperature on the Sanjiang Plain was 3.54 and 3.81 °C in 2000 and 2005, and annual precipitation was 534.6 and 542.9 mm, respectively. As there was no obvious change in climatic factors between 2000 and 2005, the most important reason for total NPP reduction must be land cover and land use changes. As described above, the main characteristic of LUCC on the Sanjiang Plain during T1 and T2 was the transformation from forest, grassland and wetland to farmland, which directly reduced regional net primary production due to the lower mean NPP of farmland. Our results showed that mean NPP for the study region decreased nearly 6 %. The areas with decreased NPP were primarily distributed in the areas with a heavy concentration of human activity.

There were some changes in climatic factors between T2 and T3; annual mean temperatures were 3.81 °C in T2 and 3.48 °C in T3, and annual precipitation was 542.9 mm in T2 and 643.8 mm in T3. Average monthly temperature in T3 was lower than in T2, and monthly mean precipitation (643.8 mm) was higher, by 8.7 and 18.6 %, than monthly averages in T2. Consequently, NPP levels in T3 are likely to have been affected by human activities.

Results show that LUCC decreased NPP on the Sanjiang Plain and that the overall release of carbon increased over the last decade. According to the reaction equations of photosynthesis and respiration, vegetation absorbs 1.62 g CO_2 to produce 1 g carbon of dry matter and releases 1.2 g O_2 in the process. Between T1 and T2, the Sanjiang Plain ecosystems lost 0.28×10^4 Gg of carbon, equivalent to reducing the carbon sink ability by 0.45×10^4 Gg and a reduction in release of 0.34×10^4 Gg O_2. The heat contained in 1 g carbon of dry matter equals that in 0.00067 g standard coal, so 0.28×10^4 Gg NPP is equivalent to the heat loss contained in 1.88×10^3 tons of standard coal. NPP is the source of the complex food chain of the forest ecosystem and changes in land use have damaged the

environment for many plants and animals, threatening their survival. By 2010, NPP had increased by at least 731 Gg of carbon, corresponding to 1184 Gg of net dioxide carbon sequestration.

Conclusions

Assessing the environmental impact of LUCC and proposing strategies for minimizing negative environmental impacts on affected NPP is challenging. The spatial and temporal patterns of change in NPP on the Sanjiang Plain were estimated by a modified CASA model and MODIS remote sensing data.

Land cover was determined from remote sensing images in order to quantify LUCC on the Sanjiang Plain from 2000 to 2010. Dry land and forest were the two largest land-use types in this region, from 2000 to 2010. Dry land constituted 40.64, 41.61, and 41.83 %, and forest 31.20, 29.89, and 28.01 %, of the total area in 2000, 2005 and 2010, respectively. The most notable changes in land use were a decline in wetland and an increase in farmland. The total area of wetland was estimated to have decreased substantially, by about 33 % to 7075 km^2; and the area of paddy field increased by about 53 %, from 11,420 km^2 in 2000 to 17,451 km^2 in 2010.

Total NPP on the Sanjiang Plain declined by 6.7 % (0.29×10^4 Gg C) from 2000 to 2005. This reduction had a significant correlation with LUCC in terms of wetland degeneration, forest reduction, and farmland increase. The main mechanism for the effect of LUCC on NPP was the transformation from wetland and forest to farmland, which is closely linked to the process of extensive land development and a large increase in migration. The largest contributor to the reduction of NPP was the conversion of forest to dry land, accounting for 54.3 % of the total NPP reduction. The likely impact of inundation and urbanization on NPP change were estimated to be 28.0 and 5.8 % of the total reduction, respectively.

The implementation of major national ecological projects on the Sanjiang Plain since 2003, however, has

significantly counteracted the negative impact of the LUCC on NPP in the region, as reflected by an emerging upward trend in NPP since 2005. This success demonstrates that ecological engineering programs can effectively rehabilitate ecosystems where the landscape and resettlement have both been altered by large development projects.

References

Ahi DE, Gower ST, Mackay DS, Burrows SN, Norman JM, Diak GR (2005) The effects of aggregated land cover data on estimating NPP in northern Wisconsin. Remote Sens Environ 97(1):1–14

Allen RG, Pereira LS, Raes D, Smith M (1998) Crop evapotranspiration: guidelines for computing crop water requirements. FAO Irrig. and Drain. Paper No. 56. United Nations FAO, Rome, Italy

Chen B, Wang SQ, Liu RG, Song T (2007) Study on modeling and spatial pattern of net primary production in China's Terrrestrial ecosystem. Resour Sci 29(6):45–53

Cramer W, Kicklighter DW, Bondeau A, Iii BM, Churkina G, Nemry B, Ruimy A, Schloss AL, Intercomparison TP (1999) Comparing global models of terrestrial net primary productivity (NPP): overview and key results. Glob Change Biol 5:1–15

DeFries RS, Field CB, Fung I, Collatz GJ, Bounoua L (1999) Combining satellite data and biogeochemical models to estimate global effects of human-induced land cover change on carbon emissions and primary productivity. Global Biogeochem Cycles 13(3):803–815

Dong GT, Yang ST, Bai J, Wang ZW, Zhang YC (2013) Open innovation in the Sanjiang Plain: a new paradigm for developing agriculture in China. J Food Agric Environ 11(3&4):1108–1113

Donmez C, Berberoglu S, Curran PJ (2011) Modelling the current and future spatial distribution of NPP in a Mediterranean watershed. Int J Appl Earth Obs Geoinf 13(3):336–345

Fang JY, Piao Shilong, Field Christopher B, Pan Yude, Guo Qinghua, Zhou Liming, Peng Changhui, Tao Shu (2003) Increasing net primary production in China from 1982 to 1999. Front Ecol Environ 1:293–297

Field CB, Randerson JT, Malmstrom CM (1995) Global net primary production: combining ecology and remote sensing. Remote Sens Environ 51(1):74–88

Guo ZX, Wang ZM, Liu DW, Song KS, Song CC (2009) Analysis of temporal and spatial features of farmland productivity in Sanjiang plain. Trans Chin Soc Agric Eng 25(1):249–254

Haxeltine A, Prentice IC (1996) BIOME3: an equilibrium terrestrial biosphere model based on ecophysiological constraints, resource availability and competition among plant functional types. Global Biogeochem Cycles 10:693–709

He Y, Dong WJ, Ji JJ, Dan L (2005) The net primary production simulation of terrestrial ecosystems in China by AVIM. Adv Earth Sci 20(3):345–349

Houghton RA (2003) Why are estimates of the terrestrial carbon balance so different? Glob Change Biol 9(4):500–509

Imhoff ML, Bounoua L, DeFries R, Lawrence WT, Stutaer D, Tucker CJ, Ricketts T (2004) The consequences of urban land transformation on net primary productivity in the United States. Remote Sens Environ 89(4):434–443

Lieth H, Whittaker RH (1975) Primary productivity of the biosphere. Springer, New York, pp 237–263

Liu J, Chen JM, Cihlar J, Parl WM (1997) A process-based boreal ecosystem productivity simulator using remote sensing inputs. Remote Sens Environ 62(2):158–175

Lobell DB, Hicke JA, Asner GP, Field CB, Tucker CJ, Los SO (2002) Satellite estimates of productivity and light use efficiency in the United States agriculture 1982–98. Glob Change Biol 8(8):722–735

Luck GW (2007) The relationships between net primary productivity, human population density and species conservation. J Biogeogr 34(2):201–212

Luo L, Wang ZM, Song KS, Ren CY, Zhang B, Liu D (2010) Research on farmland productivity about spatial-temporal features and influential factors in Songnen plain from 2000 to 2006. Syst Sci Compr Stud Agric 26(4):468–474

McCrady RL, Jokela EJ (1998) Canopy dynamics, light interception, and radiation use efficiency of selected loblolly pine families. For Sci 44:64–72

Monteith JL (1972) Solar radiation and productivity in tropical ecosystems. J Appl Ecol 9(3):747–766

Parton WJ, Scurlock JM, Ojima DS, Gilmanov TG, Scholes RJ, Schimel DS, Kirchner T, Menaut JC, Seastedt T, Garcia Moya E, Kamnalrut A, Kinyamario JL (1993) Observations and modeling of biomass and soil organic matter dynamics for the grasslands biome world-wide. Global Biochem Cycles 7:785–809

Paruelo JM, Epstei HE, Lauenroth WK, Burkei C (1997) A NPP estimates from NDVI for the central grassland region of the United States. Ecology 78:953–958

Peng CH (2000) From static biogeographical model to dynamic global vegetation model: a global perspective on modelling vegetation dynamics. Ecol Model 135(1):33–54

Piao SL, Fang JY, Guo QH (2001) Application of CASA model to the estimation of Chinese terrestrial net primary productivity. Acta Phytoecol Sinica 25(5):603–608

Piao SL, Fang JY, Zhou LM, Zhu B, Tan K, Tao S (2005) Changes in vegetation net primary productivity from 1982 to 1999 in China. Global Biogeochem Cycles 19:GB2027. doi:10.1029/2004GB002274

Pimm SL, Raven P (2000) Biodiversity-extinction by numbers. Nature 403(6772):843–845

Potter CS, Randerson JT, Field CB, Matson PA, Vitousek PM, Mooney HA, Klooster SA (1993) Terrestrial ecosystem production: a process model based on global satellite and surface data. Global Biogeochem Cycles 7(4):811–841

Potter C, Davidson E, Nepstad D, Carvalho CR (2001) Ecosystem modeling and dynamic effects of deforestation on trace gas fluxes in Amazon tropical forests. For Ecol Manage 152(1–3):97–117

Prince SD (1991) A model of regional primary production for use with coarse resolution satellite data. Int J Remote Sens 12(6):1313–1330

Prince SD, Goward SN (1995) Global primary production: a remote sensing approach. J Biogeogr 22:815–835

Quaife T, Quegan S, Disney M, Lewis P, Lomas M, Woodward FI (2008) Impact of land cover uncertainties on estimates of biospheric carbon fluxes. Global Biogeochem Cycles 22(40):GB4016. doi:10.1029/2007GB003097

Ruimy A, Saugier B (1994) Methodology for the estimation of terrestrial net primary production from remotely sensed data. J Geophys Res 97:18515–18521

Ruimy A, Dedieu G, Saugier B (1996) TURC: a diagnostic model of continental gross primary productivity and net primary productivity. Global Biogeochem Cycles 10(2):269–285

Running SW, Thornton PE, Nemani RR, Glassy JM (2000) Global terrestrial gross and net primary productivity from the earth observing system. In: Sala O, Jackson R, Mooney H (eds) Methods in ecosystem science. Springer, New York, pp 44–57

Running SW, Nemani RR, Heinsch FA, Zhao MS, Reeves M, Hashimoto H (2004) A continuous satellite-derived measure of global terrestrial primary production. Bioscience 54(6):547–560

San José J, Montes R, Grace J, Nikonoval N (2008) Land-use changes alter CO2 flux patterns of a tall-grass Andropogon field and a savanna–woodland continuum in the Orinoco lowlands. Tree Physiol 28(3):437–450

Schimel DS, Participants V, Braswell BH (1997) Continental scale variability in ecosystem processes: models, data, and the role of disturbance. Ecol Monogr 67:251–271

Seixas J, Carvalhais N, Nunes C, Benali A (2009) Comparative analysis of MODIS-FAPAR and MERIS-MGVI datasets: potential impacts on ecosystem modeling. Remote Sens Environ 113(12):2547–2559

Song KS, Liu DW, Wang ZM, Zhang B, Jin C, Li F, Liu HJ (2008) Land use change in Sanjiang Plain and its driving forces analysis since 1954. Acta Geographica Sinica 63(1):93–104

Tao FL, Yokozawa M, Zhang Z, Xu YL, Hayashi Y (2005) Remote sensing of crop production in China by production efficiency models: models comparisons, estimates and uncertainties. Ecol Model 183(4):385–396

Williams JW, Seabloom EW, Slayback D, Stoms DM, Viers JH (2005) Anthropogenic impacts upon plant species richness and net primary productivity in California. Ecol Lett 8(2):127–137

Xu C, Liu M, An S, Chen JM, Yan P (2007) Assessing the impact of urbanization on regional net primary productivity in Jiangyin County, China. J Environ Manage 85(3):597–606

Yu DY, Shao HB, Pj Shi, Zhu WQ, Pan YZ (2009) How does the conversion of land cover to urban use affect net primary productivity? A case study in Shenzhen city, China. Agric For Meteorol 149(11):2054–2060

Zhang F, Zhou GS (2008) Spatial-temporal variations in net primary productivity along Northesat China Transect (NECT) from 1982 to 1999. J Plant Ecol (Chinese version) 32(4):798–809

Zhu WQ, Pan YZ, He H, Yu DY, Hu HB (2006) Simulation of maximum light use efficiency for some typical vegetation types in China. Chin Sci Bull 51(4):457–463

Zhu WQ, Pan YZ, Zhang JS (2007) Estimation of net primary productivity of Chinese vegetation based on remote sensing. Acta Phytoecol Sinica 31(3):413–424

Zika M, Erb KH (2009) The global loss of net primary production resulting from human-induced soil degradation in drylands. Ecol Econ 69(2):310–318